



RESEARCH LETTER

10.1002/2015GL067487

Key Points:

- Rayleigh waves instantly induce the colocated infrasonic waves
- Traveling seismo-atmosphere disturbances travel with the sound speed
- Apply the circle method on seismo-generated infrasonic waves

Correspondence to:

J. Y. Liu,
jyliu@jupiter.ss.ncu.edu.tw

Citation:

Liu, J. Y., et al. (2016), The vertical propagation of disturbances triggered by seismic waves of the 11 March 2011 M9.0 Tohoku earthquake over Taiwan, *Geophys. Res. Lett.*, *43*, 1759–1765, doi:10.1002/2015GL067487.

Received 17 DEC 2015

Accepted 1 FEB 2016

Accepted article online 4 FEB 2016

Published online 24 FEB 2016

The vertical propagation of disturbances triggered by seismic waves of the 11 March 2011 M9.0 Tohoku earthquake over Taiwan

J. Y. Liu^{1,2}, C. H. Chen³, Y. Y. Sun², C. H. Chen⁴, H. F. Tsai⁴, H. Y. Yen⁵, J. Chum⁶, J. Lastovicka⁶, Q. S. Yang¹, W. S. Chen⁷, and S. Wen⁸

¹College of Mechanical Engineering and Applied Electronics Technology, Beijing University of Technology, Beijing, China,

²Institute of Space Science, National Central University, Taoyuan, Taiwan, ³Department of Earth and Environmental

Sciences, National Chung Cheng University, Chiayi, Taiwan, ⁴Department of Earth Sciences, National Cheng Kung

University, Tainan, Taiwan, ⁵Institute of Geophysics, National Central University, Taoyuan, Taiwan, ⁶Institute of Atmospheric

Physics ASCR, Prague, Czech Republic, ⁷Institute of Earthquake Prediction, Beijing University of Technology, Beijing, China,

⁸National Center for Research on Earthquake Engineering, Taipei, Taiwan

Abstract In this paper, concurrent/colocated measurements of seismometers, infrasonic systems, magnetometers, HF-CW (high frequency-continuous wave) Doppler sounding systems, and GPS receivers are employed to detect disturbances triggered by seismic waves of the 11 March 2011 M9.0 Tohoku earthquake. No time delay between colocated infrasonic (i.e., super long acoustic) waves and seismic waves indicates that the triggered acoustic and/or gravity waves in the atmosphere (or seismo-traveling atmospheric disturbances, STADs) near the Earth's surface can be immediately activated by vertical ground motions. The circle method is used to find the origin and compute the observed horizontal traveling speed of the triggered infrasonic waves. The speed of about 3.3 km/s computed from the arrival time versus the epicentral distance suggests that the infrasonic waves (i.e., STADs) are mainly induced by the Rayleigh waves. The agreements in the travel time at various heights between the observation and theoretical calculation suggest that the STADs triggered by the vertical motion of ground surface caused by the Tohoku earthquake traveled vertically from the ground to the ionosphere with speed of the sound in the atmosphere over Taiwan.

1. Introduction

Vertical motions of the Earth's surface, due to earthquakes creating mechanical disturbances, trigger acoustic and/or gravity waves in the neutral atmosphere near the Earth's surface (hereafter termed, seismo-traveling atmospheric disturbances (STADs)), which propagate into the ionosphere and interact with the ionized gas, (see papers listed in Davies [1990]). Traditionally, seismometers record seismic waves monitoring the Earth's surface motion [Shearer, 1999], and infrasonic systems measure atmospheric pressure changes (or STADs) induced by the Earth's surface motion and/or seismic waves, mainly Rayleigh waves, on the ground [Mutschlecner and Whitaker, 2005]. The triggered STADs then travel upward through the lower ionosphere significantly modifying the Hall and Pedersen conductivity at the peak height of about 105–110 km altitude [Kelley, 2009] and in turn affecting the Earth's magnetic field [Hao et al., 2013; Chen et al., 2014; Yen et al., 2015]. In fact, the STADs often continue traveling upward into the ionosphere and perturbing the plasma density within it, which is termed seismo-traveling ionospheric disturbances (STIDs). Scientists have reported STIDs in the frequency shift of HF-CW (high frequency-continuous wave) Doppler sounding systems [Liu et al., 2006; Chum et al., 2012], the total electron content (TEC) derived by ground-based GPS receivers [Ducic et al., 2003; Artru et al., 2004; Jung et al., 2006; Liu et al., 2011; Tsai et al., 2011], and vertical electron density profiles of the space-based GPS occultation experiment on board the FORMOSAT-3/COSMIC satellite [Sun et al., 2015]. Thus, magnetometers, HF-CW Doppler sounding systems, and GPS receivers can be used to observe STIDs at the ionospheric conducting layer at 100 ± 20 km altitude [cf. Yen et al., 2015], the reflection point of the Doppler sounding signal of 5.26 MHz at about 200 ± 20 km altitude [Liu et al., 2006], and the ionospheric point of the GPS signal at 350 ± 50 km altitude [cf. Liu et al., 1996, 2011; Tsai et al., 2011], respectively.

Many studies report STIDs triggered by the 11 March 2011 M9.0 Tohoku earthquake by means of ionospheric TEC derived from ground-based GPS receivers [Chen et al., 2011; Liu et al., 2011; Maruyama et al., 2011; Rolland et al., 2011; Tsai et al., 2011] and ionograms of ionosondes [Liu and Sun, 2011; Maruyama et al., 2011]. The

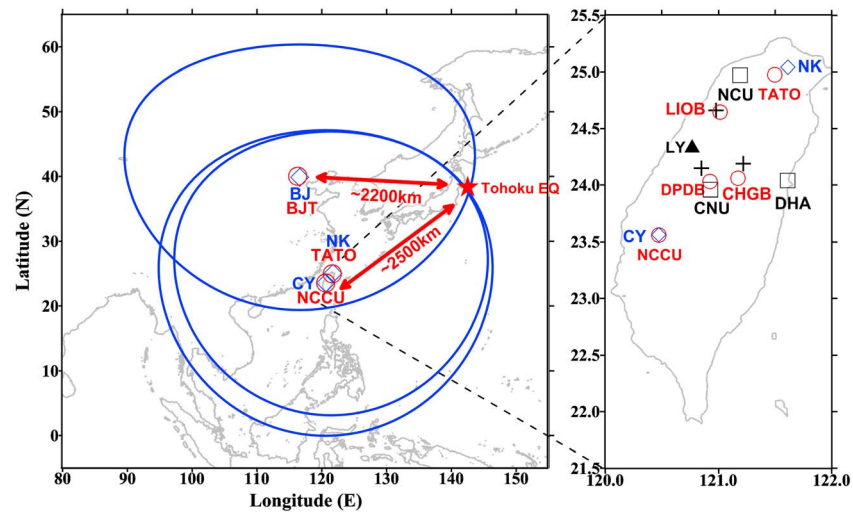


Figure 1. Locations of seismometers (red circles), infrasonic systems (blue diamonds), a magnetometer at LY (the black triangle), ionospheric reflection points (black crosses) of the Doppler sounding system (black squares), and GPS receiver with the subionospheric point around NCU. The blue annuluses in the left panel are the products of the traveling time and the assumed speed at BJ, NK, and CY.

horizontal propagation of the triggered STID has been examined in somewhat detailed. However, due to solo or limited collocated instruments being available, scientists cannot study the vertical propagation in detail but simply find the travel time(s) at a (few) certain altitude(s). Therefore, in this paper, five different measurements of seismometers, infrasonic systems, total field magnetometers, HF-CW Doppler sounding systems with sounding frequency at 5.26 MHz, and GPS receivers on the ground are used to monitor the ground motion, STADs in the near Earth's surface atmosphere, and the associated STIDs at about 100, 200, and 350 km altitude, respectively, triggered by the 11 March 2011 *M*9.0 Tohoku earthquake. Data recorded by infrasonic systems in Taiwan and China are employed to confirm whether the STADs are generated by the seismic waves. The collocated five instruments in the northern Taiwan are used to find the travel times at various altitudes and investigate the vertical propagation of the generated STADs and/or STIDs. The speed and travel time for acoustic waves vertically traveling from the ground to the ionosphere are theoretically computed [Zuckerwar, 2002] and cross compared with those collocated observations.

2. Observation and Interpretation

A magnitude *M*9.0 earthquake occurred at 05:46:23 UTC on 11 March 2011; the epicenter was located at 38.322°N, 142.369°E off the east coast of Honshu, Japan, and was reported by the U.S. Geological Survey (<http://earthquake.usgs.gov/earthquakes/eqinthenews/2011/usc0001xgp/>). We examine measurements recorded by the five different instruments in Taiwan and China to understand the link of disturbances, seismic waves on the ground, STADs in the atmosphere, and STIDs in the ionosphere, excited by the 11 March 2011 *M*9.0 Tohoku earthquake. Figure 1 displays locations of six seismometers, three infrasound sensors, one magnetometer, three reflection points of the HF-CW Doppler sounding system, and one ground-based GPS receiver. The data sampling rate of these measurements is 1 Hz. Figure 2 illustrates raw data of the collocated pairs of seismograms-infrasonic waves and seismograms-Doppler frequency shifts during the Tohoku earthquake. Here the term "collocated" is defined as the horizontal distance from the reference seismometer to the infrasonic sensor, the magnetometer, the Doppler reflection point, and the ionospheric GPS point is one half shorter than their associated altitudes of 0 km, 50 km, 100 km, and 175 km, respectively. Since Taiwan is about 3000 km away from the epicenter, the horizontal wavelength of the arriving seismic waves (especially from the wave packet view point) is rather long, which in turn results in the vertical motions of the Earth's surface at various locations in Taiwan being nearly in phase. Thus, the nearby instruments may be treated as collocated, and the STADs can travel upward almost unattenuatedly.

It can be seen that there is no clear earthquake signature in the raw records of infrasonic waves, while three distinct Doppler frequency shifts lag the associated seismic waves by about 500 s. The compact packets of short-period signals are observed in the seismograms in Taiwan and in Beijing, China, where are about 3000 km and

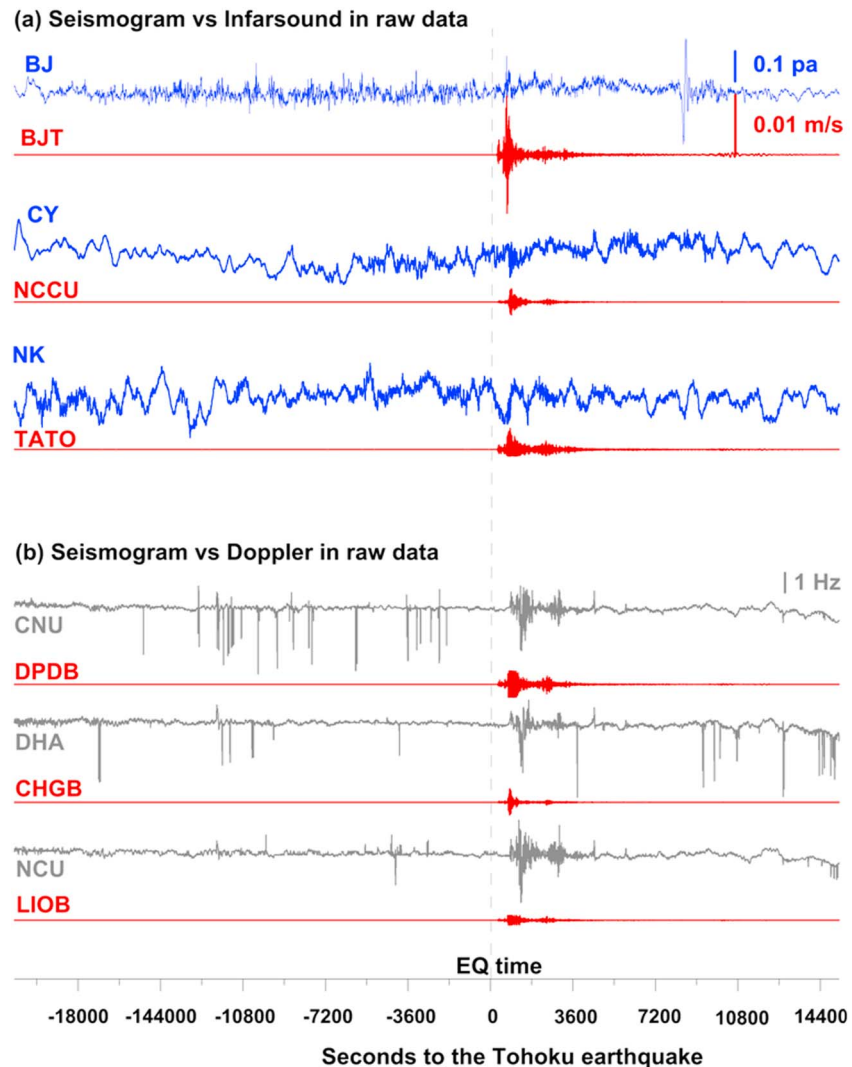


Figure 2. Raw data of colocated pairs of (a) seismograms and infrasonic waves as well as (b) seismograms and Doppler shifts during the Tohoku earthquake period.

2600 km away from the epicenter, at about 900 s and 750 s after the earthquake, respectively. This suggests that prominent Rayleigh waves with average speeds of 3.2–3.3 km/s have been observed. To clearly see the STAD and STID signatures, high-pass filtering processes have been applied. Note that the differential quantities of seismograms (i.e., velocities), infrasonic fluctuations, and Doppler frequency shifts are more sensitive to higher frequencies, while the integral quantities of magnetic total fields and GPS TECs have better response to relatively lower frequencies. Therefore, the differential and integral quantities are examined by means of the Fourier transform analysis with high-pass filters of 30 s and 300 s, respectively. It is found that filtered fluctuations of the colocated seismograms-infrasonic waves are nearly identical (Figure 3a). A cross correlation shows that the packet of the seismic waves tends to lead that of the associated Doppler frequency shifts by about 498–516 s (Figure 3b). To understand the seismic and associated infrasonic waves, the circle method [Lay and Wallace, 1995] is applied. In Figure 1, three circles are drawn with the radius of 3.2–3.3 km/s multiplied by the associated arrival times of about 600 s, 720 s, and 750 s from the centers at BJ/BJT, NK/TATO, and CY/NCCU, respectively. The intersection of the three circles coincides with the Tohoku epicenter, which suggests that the STADs reported in this study are most likely induced by the Rayleigh waves of the Tohoku earthquake.

To study the vertical propagation of the triggered STADs/STIDs, measurements of seismic waves at TATO, infrasonic waves at NK, magnetic field fluctuations near LY, Doppler frequency shifts recorded at NCU, and

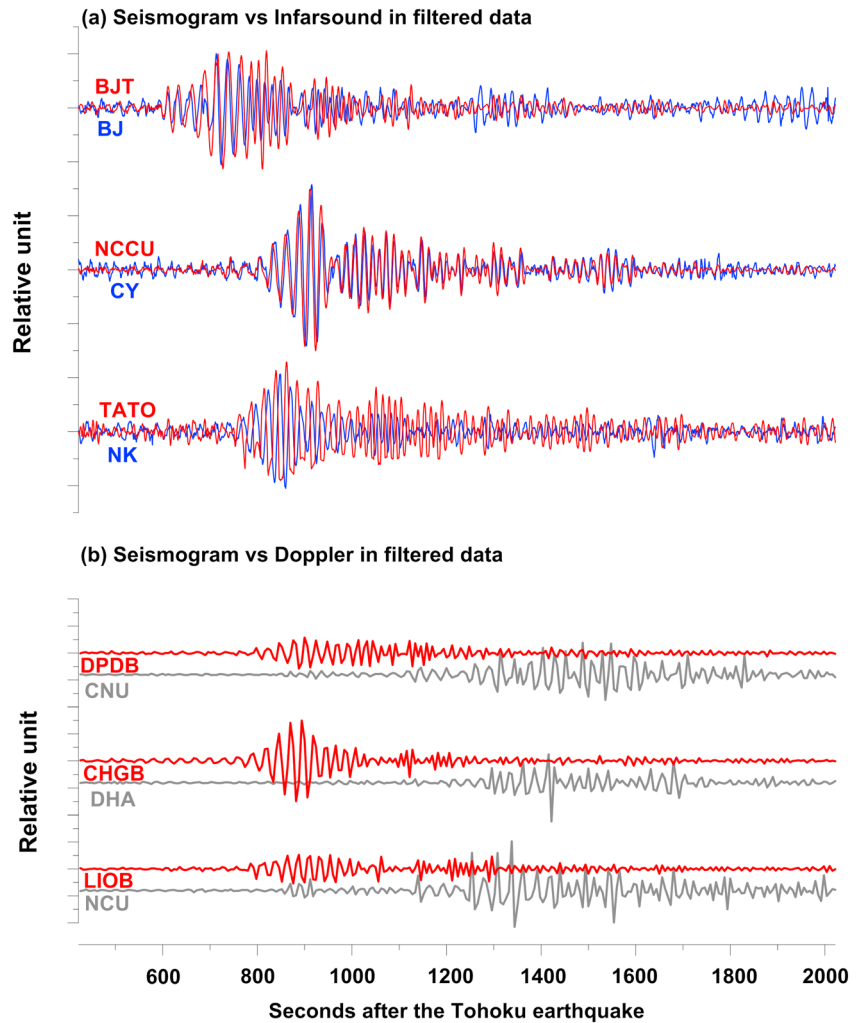


Figure 3. Data in Figure 2 filtered with a band pass of 30–300 s. (a) Seismograms and infrasonic waves and (b) seismograms and Doppler shift.

GPS TEC at around subionospheric point NCU in Taiwan are analyzed. A high-pass filter of 300 s in period is applied on fluctuations in the geomagnetic total intensity field with 1 Hz and 0.01 nT resolution and those in the rate of change in the TEC (rTEC) [Liu et al., 2004] derived from the GPS satellite (pseudorandom noise (PRN) 18) with 1 s sampling rate. The filtered fluctuation packet of the seismic waves is further used to cross correlate with that of the geomagnetic total intensity field, Doppler frequency shift, and GPS TEC accordingly. Figure 4 reveals that the seismic and infrasonic waves generally coincide with each other. The fluctuation packets of the two coincidentally appear at about 870 s after the Tohoku earthquake. The cross correlation shows that the fluctuation packet of the seismic waves leads that of the magnetic field, Doppler frequency shift, and rTEC by about 400 ± 269 s, 516 ± 416 s, and 836 ± 256 s, respectively.

The sound speed in the ideal gas (C_s) is

$$C_s = \sqrt{\frac{\gamma RT}{M}}, \tag{1}$$

where γ (7/5) is the adiabatic index and R ($8.3145 \text{ J} \cdot \text{mol}^{-1} \cdot \text{K}^{-1}$) is the molar gas constant. The molecular weight (M) and the absolute temperature (T) are obtained from the Naval Research Laboratory Mass Spectrometer Incoherent Scatter Radar model [Picone et al., 2002]. Based on C_s obtained from equation (1),

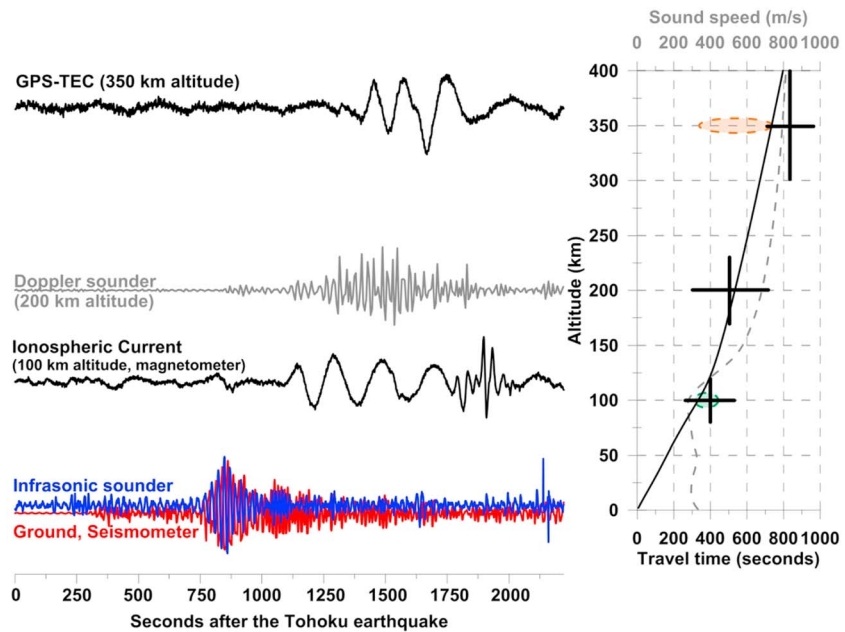


Figure 4. Colocated filtered data of the five data observed at Taiwan area and travel times for vertically propagating infrasound waves. Here the ionospheric conducting layer at 100 ± 20 km altitude, the reflection point of the Doppler sounding frequency at 200 ± 30 km altitude, and the ionospheric point of a ground-based GPS receiver at the 350 ± 50 km altitude are based on magnetometer studies [Hao *et al.*, 2013; Chen *et al.*, 2014; Yen *et al.*, 2015], the Doppler sounding observations in Taiwan [Liu *et al.*, 2006], and ionospheric GPS signal studies [Liu *et al.*, 1996], respectively. The seismo-magnetic pulsations lag the seismic wave pulses by about 378 ± 62 s [Yen *et al.*, 2015] (green oval), while the GPS TEC fluctuations appear the seismic wave pulses by about 540 ± 200 s [Tsai *et al.*, 2011] (orange oval).

we computed the travel time t_p of an acoustic wave propagating upward from the ground to different heights h in the ionosphere (red curve in the right plot in Figure 4) as

$$t_p = \int_0^h \frac{dz}{c_s} \tag{2}$$

It is interesting to find that the travel time of the theoretical calculation generally agrees with that observed at 100 km altitude around the peak of the Hall and Pedersen conductivities, at 200 km altitude of the reflection point of the Doppler sounding signals, and at 350 km altitude of the ionospheric point of the GPS signals (see Figure 4). This result confirms the observations by Chum *et al.* [2012] who found from continuous Doppler sounding that the observation of infrasound wave packets in the ionosphere at altitude of about 210 km followed the arrival of seismic wave packets with delays of about 9 min, which was in agreement with theoretically calculated times for vertically propagating infrasound waves. The acoustic speed of vertical propagation was also confirmed by the study of Maruyama and Shinagawa [2014] based on the detailed analysis of ionograms measured in Japan at distances longer than ~ 800 km from the epicenter.

3. Discussion and Conclusion

Many papers study STIDs induced by the 11 March 2011 M9.0 Tohoku earthquake. Liu *et al.* [2011] report that STIDs of the GPS TEC first appear near the epicenter about 7 min after the Tohoku earthquake onset, while Tsai *et al.* [2011] find that the STIDs in GPS TEC triggered by the Rayleigh waves appear 7–8 min after the earthquake occurrence. On the other hand, Liu and Sun [2011] estimate that the travel time of STIDs in ionograms from the ground to the ionosphere at about 200 km altitude is about 4 min. Maruyama *et al.* [2011] further cross compare concurrent/colocated GPS TECs and ionograms recorded by the four ionosondes in Japan during the Tohoku earthquake. They find the earlier onset of the disturbance in the ionogram than the commencement of the propagating TEC perturbation. Since fluctuations in TEC are sensitive to the disturbance near the F_2 peak (about 350 km altitude), while the observed ionosonde STIDs are at the reflection

height of about 200 km altitude, the 4 min time lag should be reasonable for the STIDs directly and/or locally triggered by seismic waves under them. Although the above studies show that the average speeds from the ground to the ionosphere at 200 and 350 km altitude are about 830 and 730–830 m/s, respectively, it is difficult to find whether the STADs were triggered and then vertically traveled into the ionosphere resulting in the STIDs within it, even though the value of speed supports rather acoustic waves (infrasound). In fact, it is even more surprising to find that in this study, vertical travel times of the Doppler frequency shift and rTEC from the ground to the ionosphere at about 200 km and 350 km altitude are about 516 s and 836 s (i.e., 8.6 min and 13.9 min), respectively. Note that they are much farther away than those observed near the epicenter area reported by the previous researches. It is known that on the ground, the vertical displacement is 2–5 m above the source rupture area [Maeda et al., 2011], while that in Taiwan should be less than 5 cm [Hung and Rau, 2013]. The vertical scale of the disturbances is 10–30 km in the lower part of the ionosphere [Maruyama et al., 2012], and it may be much greater in higher altitude [Liu et al., 2012], which may shorten the travel time from the ground to the ionosphere near the epicenter and/or the tsunami origin. Astafyeva et al. [2011] reported that the first TEC disturbances appeared 464 s after the earthquake beginning. At that time, the acoustic waves could not reach the altitude of maximum ionization (more than 250 km). Thus, it is probable that the first ionospheric perturbations were caused by shock-acoustic waves that carried the majority of available electrons, possibly propagating at supersonic speed at low altitudes [Astafyeva et al., 2011].

Yen et al. [2015] examine geomagnetic pulsations recorded by a wide-area network of 12 magnetometers excited by traveling Rayleigh waves of the 2011 M9.0 Tohoku-oki earthquake. They find that seismo-magnetic pulsations constantly lag seismic wave pulses by about 6.3 min ($=378 \pm 62$ s), which is within the range of 400 ± 269 s reported in this paper. Since these magnetometers generally are far away from the epicenter, the travel time of Yen et al. [2015] and that observed and theoretically calculated in this study are all in good agreements (see Figure 4).

On the other hand, Tsai et al. [2011] compute the mean horizontal speed of 2.3 km/s along the surface by using 29 TEC of GPS satellite-receiver pairs, which agrees with the Rayleigh wave speed, and the linear regression shows that the STADs/STIDs traveling from the ground to the right above subionospheric point at 350 km altitude about 9 min (540 ± 180 s). A large portion of their data is collected around the epicenter, and therefore, the travel time estimated by the linear regression in Tsai et al. [2011] should be shorter, which can be also seen in Figure 4. Nevertheless, the travel time of Tsai et al. [2011] and that observed and theoretically calculated in this study are all in agreements. These agreements once again indicate that the STADs are mainly induced by the traveling Rayleigh waves and travel with the sound speed in upward direction.

The nearly identical fluctuations of the collocated seismograms-infrasound waves and the coincidence of the intersection of the three circles with the Tohoku epicenter confirms that the STADs near the Earth's surface are prominently induced by the Rayleigh waves of the Tohoku earthquake. The agreement between the theoretical calculation and the collocated observation suggests that the STADs induced by seismic waves in Taiwan area, sufficiently far from the epicentral area, vertically travel from the ground to the ionosphere with the sound speed. Application of various types of data and methods of measurements at Taiwan made it possible for the first time to track the vertical propagation of acoustic/infrasound waves (i.e., STADs) from their excitation by seismic oscillations at surface documented by infrasound measurements through ionospheric E (i.e., magnetometer) and F regions (i.e., Doppler frequency shift) up to the upper ionosphere (i.e., rTEC).

Acknowledgments

This study is supported by the project 41474138 of National Natural Science Foundation of China; the grant MOST104-2923-M-008-002-MY3, Taiwan-Czech Joint Research Cooperation, by the Ministry of Science and Technology; the grant 15-07281 J by the Czech National Foundation and the project M100421201 of the Czech Academy of Sciences; and the grant 2012BAK29B01 of the National Key Technology R&D Program. Seismometer/magnetometer and infrasound/HF Doppler shift/GPS TEC data were purchased from Central Weather Bureau (<http://www.cwb.gov.tw/eng/index.htm>) and Graduate Institute of Space Science, National Central University (<http://www.ss.ncu.edu.tw/>), respectively.

References

- Artru, J., T. Farges, and P. Lognonné (2004), Acoustic waves generated from seismic surface waves: Propagation properties determined from Doppler sounding observations and normal-mode modelling, *Geophys. J. Int.*, *158*, 1067–1077, doi:10.1111/j.1365-246X.2004.02377.
- Astafyeva, E., P. Lognonné, and L. Rolland (2011), First ionospheric images of the seismic fault slip on the example of the Tohoku-oki earthquake, *Geophys. Res. Lett.*, *38*, L22104, doi:10.1029/2011GL049623.
- Chen, C. H., A. Saito, C. H. Lin, J. Y. Liu, H. F. Tsai, T. Tsugawa, Y. Otsuka, M. Nishioka, and M. Matsumura (2011), Long-distance propagation of ionospheric disturbance generated by the 2011 off the Pacific coast of Tohoku Earthquake, *Earth Planets Space*, *63*, 881–884, doi:10.5047/eps.2011.06.026.
- Chen, C. H., C. H. Wang, L. C. Lin, H. H. Hsieh, H. Y. Yen, and M. H. Shih (2014), Typhoon-induced magnetic disturbances: Cases in the Western Pacific, *Terr. Atmos. Oceanic Sci.*, *25*, 647–653, doi:10.3319/TAO.2014.05.08.01(AA).
- Chum, J., F. Hruska, J. Zednik, and J. Lastovicka (2012), Ionospheric disturbances (infrasound waves) over the Czech Republic excited by the 2011 Tohoku earthquake, *J. Geophys. Res.*, *117*, A08319, doi:10.1029/2012JA017767.
- Davies, K. (1990), *Ionospheric Radio*, pp. 580, Peter Peregrinus Ltd., London.

- Ducic, V., J. Artru, and P. Longnonne (2003), Ionospheric remote sensing of the Denali earthquake Rayleigh surface wave, *Geophys. Res. Lett.*, *30*(18), 1951, doi:10.1029/2003GL017812.
- Hao, Y. Q., Z. Xiao, and D. H. Zhang (2013), Teleseismic magnetic effects (TMDs) of 2011 Tohoku earthquake, *J. Geophys. Res. Space Physics*, *118*, 3914–3923, doi:10.1002/jgra.50326.
- Hung, H.-K., and R.-J. Rau (2013), Surface waves of the 2011 Tohoku earthquake: Observations of Taiwan's dense high-rate GPS network, *J. Geophys. Res. Solid Earth*, *118*, 332–345, doi:10.1029/2012JB009689.
- Jung, T. K., J. Y. Liu, H. F. Tsai, B. S. Huang, C. H. Lin, S. B. Yu, and Y. S. Yeh (2006), Ionospheric disturbances triggered by the M_w 7.6 earthquake off the coast of El Salvador on 13 January 2001, *Terr. Atmos. Oceanic Sci.*, *17*, 345–351.
- Kelley, M. (2009), *The Earth's Ionosphere: Plasma Physics and Electrodynamics*, 2nd ed., Academic Press, San Diego, Calif.
- Lay, T., and T. C. Wallace (1995), *Modern Global Seismology*, San Diego, Calif.
- Liu, J. Y., and Y. Y. Sun (2011), Seismo-traveling ionospheric disturbances of ionograms observed during the 2011 M_w 9.0 Tohoku earthquake, *Earth Planets Space*, *63*, 897–902, doi:10.5047/eps.2011.05.017.
- Liu, J. Y., H. F. Tsai, and T. K. Jung (1996), Total electron content obtained by using the global positioning system, *Terr. Atmos. Oceanic Sci.*, *7*, 107–117.
- Liu, J. Y., C. H. Lin, H. F. Tsai, and Y. A. Liou (2004), Ionospheric solar flare effects monitored by the ground-based GPS receivers: Theory and observation, *J. Geophys. Res.*, *109*, A01307, doi:10.1029/2003JA009931.
- Liu, J. Y., Y. B. Tsai, S. W. Chen, C. P. Lee, Y. C. Chen, H. Y. Yen, W. Y. Chang, and C. Liu (2006), Giant ionospheric disturbances excited by the M 9.3 Sumatra earthquake of 26 December 2004, *Geophys. Res. Lett.*, *33*, L02103, doi:10.1029/2005GL023963.
- Liu, J. Y., C. H. Chen, C. H. Lin, H. F. Tsai, C. H. Chen, and M. Kamogawa (2011), Ionospheric disturbances triggered by the 11 March 2011 M 9.0 Tohoku earthquake, *J. Geophys. Res.*, *116*, A06319, doi:10.1029/2011JA016761.
- Liu, J. Y., Y. Y. Sun, H. F. Tsai, and C. H. Lin (2012), Seismo-traveling ionospheric disturbances triggered by the 12 May 2008 M 8.0 Wenchuan Earthquake, *Terr. Atmos. Oceanic Sci.*, *23*, 9–15, doi:10.3319/TAO.2011.08.03.01(T).
- Maeda, T., T. Furumura, S. Sakai, and M. Shinohara (2011), Significant tsunami observed at the ocean-bottom pressure gauges at 2011 off the Pacific coast of Tohoku earthquake, *Earth Planets Space*, *63*, 803–808, doi:10.5047/eps.2011.06.005.
- Maruyama, T., and H. Shinagawa (2014), Infrasonic sounds excited by seismic waves of the 2011 Tohoku-oki earthquake as visualized in ionograms, *J. Geophys. Res. Space Physics*, *119*, 4094–4108, doi:10.1002/2013JA019707.
- Maruyama, T., T. Tsugawa, H. Kato, A. Saito, Y. Otsuka, and M. Nishioka (2011), Ionospheric multiple stratifications and irregularities induced by the 2011 Tohoku earthquake, *Earth Planets Space*, *63*(7), 869–873, doi:10.5047/eps.2011.06.008.
- Maruyama, T., T. Tsugawa, H. Kato, M. Ishii, and M. Nishioka (2012), Rayleigh wave signature in ionograms induced by strong earthquakes, *J. Geophys. Res.*, *117*, A08306, doi:10.1029/2012JA017952.
- Mutschlecner, J. P., and R. W. Whitaker (2005), Infrasound from earthquakes, *J. Geophys. Res.*, *110*, D01108, doi:10.1029/2004JD005067.
- Picone, J. M., A. E. Hedin, D. P. Drob, and A. C. Aikin (2002), NRLMSISE-00 empirical model of the atmosphere: Statistical comparisons and scientific issues, *J. Geophys. Res.*, *107*(A12), 1468, doi:10.1029/2002JA009430.
- Rolland, L. M., P. Lognonné, E. Astafyeva, E. A. Kherani, N. Kobayashi, M. Mann, and H. Munekane (2011), The resonant response of the ionosphere imaged after the 2011 off the Pacific coast of Tohoku earthquake, *Earth Planets Space*, *63*, 853–857, doi:10.5047/eps.2011.06.020.
- Shearer, P. M. (1999), *Introduction to Seismology*, pp. 260, Cambridge Univ. Press.
- Sun, Y.-Y., J.-Y. Liu, C.-Y. Lin, H.-F. Tsai, L. C. Chang, C.-Y. Chen, and C.-H. Chen (2015), Ionospheric F2 region perturbed by the 25 April 2015 Nepal earthquake, 2015 AGU Fall meeting, San Francisco, Calif.
- Tsai, H. F., J. Y. Liu, C. H. Lin, and C. H. Chen (2011), Tracking the epicenter and the tsunami origin with GPS ionosphere observation, *Earth Planets Space*, *63*, 859–862, doi:10.5047/eps.2011.06.024.
- Yen, H. Y., C. R. Chen, Y. T. Lo, T. C. Shin, and Q. Li (2015), Seismo-geomagnetic pulsations triggered by Rayleigh waves of the 11 March 2011 M 9.0 Tohoku-oki earthquake, *Terr. Atmos. Oceanic Sci.*, *26*, 95–101, doi:10.3319/TAO.2014.10.09.01(T).
- Zuckerwar, A. J. (2002), *Handbook of the Speed of Sound in Real Gases*, Academic Press, San Diego, Calif.